DNA Methylation Represses IFN-γ–Induced and Signal Transducer and Activator of Transcription 1–Mediated IFN Regulatory Factor 8 Activation in Colon Carcinoma Cells

Jon M. McGough,[1] Dafeng Yang,[1] Shuang Huang,[1] David Georgi,[2] Stephen M. Hewitt,[3] Christoph Röcken,[4] Marc Tänzer,[5] Matthias P.A. Ebert,[5] and Kebin Liu[1]

Departments of [1]Biochemistry and Molecular Biology and [2]Pathology, Medical College of Georgia, Augusta, Georgia; [3]Tissue Array Research Program, National Cancer Institute, NIH, Bethesda, Maryland; [4]Institute of Pathology, Charite, Universitätsmedizin, Berlin, Germany; and [5]Department of Medicine II, Klinikum rechts der Isar, Technical University of Munich, Munich, Germany

Abstract

IFN regulatory factor 8 (IRF8) is both constitutively expressed and IFN-γ inducible in hematopoietic and nonhematopoietic cells. We have shown that IRF8 expression is silenced by DNA methylation in human colon carcinoma cells, but the molecular mechanism underlying methylation-dependent IRF8 silencing remains elusive. In this study, we observed that IRF8 protein level is inversely correlated with the methylation status of the IRF8 promoter and the metastatic phenotype in human colorectal carcinoma specimens *in vivo*. Demethylation treatment or knocking down DNMT1 and DNMT3b expression rendered the tumor cells responsive to IFN-γ to activate IRF8 transcription *in vitro*. Bisulfite genomic DNA sequencing revealed that the entire CpG island of the IRF8 promoter is methylated. Electrophoresis mobility shift assay revealed that DNA methylation does not directly inhibit IFN-γ–activated phosphorylated signal transducer and activator of transcription 1 (pSTAT1) binding to the IFN-γ activation site element in the IRF8 promoter *in vitro*. Chromatin immunoprecipitation assay revealed that pSTAT1 is associated with the IFN-γ activation site element of the IRF8 promoter *in vivo* regardless of the methylation status of the IRF8 promoter. However, DNA methylation results in preferential association of PIAS1, a potent inhibitor of pSTAT1, with pSTAT1 in the methylated IRF8 promoter region. Silencing methyl-CpG binding domain protein 1 (MBD1) expression resulted in IRF8 activation by IFN-γ in human colon carcinoma cells with methylated IRF8 promoter. Our data thus suggest that human colon carcinoma cells silence IFN-γ–activated IRF8 expression through MBD1-dependent and PIAS1-mediated inhibition of pSTAT1 function at the methylated IRF8 promoter.

(Mol Cancer Res 2008;6(12):1841–51)

Introduction

IFN regulatory factor 8 (IRF8) is a central mediator in the IFN-γ/signal transducer and activator of transcription 1 (STAT1) signaling pathway and functions as a suppressor of both hematopoietic and nonhematopoietic tumors (1-4). One of the prominent phenotypes of IRF8 null mice is marked clonal expansion of undifferentiated granulocytes and macrophages. These IRF8-deficient myeloid cells frequently progress to a syndrome similar to human chronic myelogenous leukemia (2, 5, 6). In human patients with chronic myelogenous leukemia and acute myeloid leukemia, IRF8 expression is dramatically decreased (7). These studies thus revealed that IRF8 functions as a tumor suppressor of certain hematopoietic malignancies.

In an earlier study to identify differentially expressed genes between primary and metastatic colon carcinoma tumor cell lines using DNA microarray analysis, we identified that IFN-γ induces IRF8 expression in human colon carcinoma cells (i.e., nonhematopoietic tumor cells) and that IRF8 expression level is inversely correlated with the metastatic phenotype (8). Recently, we showed that IRF8 can be repressed by DNA methylation in human colon carcinoma cells. We further showed that disruption of IRF8 function or silencing IRF8 expression significantly decreased the tumor cell sensitivity to apoptosis and conferred the low metastatic tumor cells with metastatic potential in an experimental metastasis mouse model (3, 4, 9). The direct effect of IRF8 on nonhematopoietic tumor development has also been shown in various carcinoma cells (10, 11). It was shown that both constitutively expressed and IFN-γ–induced IRF8 mediates apoptosis in lens carcinoma cells, and ectopic expression of IRF8 inhibited the clonogenicity of colon, lens, esophageal, and nasopharyngeal carcinoma cells (10, 11). Furthermore, a recent study has extended the IRF8 promoter methylation to multiple human carcinomas, including nasopharyngeal, cervical, breast, and esophageal carcinoma (11). Therefore, IRF8 also functions as an apoptosis regulator and tumor suppressor in nonhematopoietic tumors and its expression is regulated by DNA methylation. In addition, analysis of expressed sequence tag data in the UniGene database of the National Center for Biotechnology Information

Received 6/13/08; revised 8/21/08; accepted 8/31/08.
Grant support: CA133085 (K. Liu) from the National Cancer Institute, NIH. M.P.A. Ebert is supported by the Else Kröner-Fresenius-Stiftung (Homburg, Germany).
The costs of publication of this article were defrayed in part by the payment of page charges. This article must therefore be hereby marked *advertisement* in accordance with 18 U.S.C. Section 1734 solely to indicate this fact.
Requests for reprints: Kebin Liu, Department of Biochemistry and Molecular Biology, Medical College of Georgia, 1459 Laney Walker Boulevard, Augusta, GA 30912. Phone: 706-721-9483; Fax: 706-721-6608. E-mail: Kliu@mcg.edu

doi:10.1158/1541-7786.MCR-08-0280

indicates that IRF8 is expressed in a broad spectrum of human tumors, including bone, colorectal, gastrointestinal, glial, kidney, respiratory tract, muscle tissue, and uterine tumors. Examination of DNA microarray data deposited in the National Center for Biotechnology Information Gene Expression Omnibus database revealed that IRF8 expression is detected in human breast, bone, soft tissue, cervix, colorectal, glial, kidney, lung, skin, ovarian, and prostate cancers. Thus, IRF8 is ubiquitously expressed in human tumors of diverse types and histologies.

Although IRF8 is constitutively expressed in macrophages, other myeloid cells, B cells, and T cells, expression of IRF8 can be dramatically up-regulated by IFN-γ (12). The relative roles of constitutively expressed IRF8 and IFN-γ–activated IRF8 are still not well defined and remain an active research area (12). IRF8 is also constitutively expressed in certain nonhematopoietic tumor cells, albeit at lower level, but its expression can also be dramatically up-regulated by IFN-γ (3, 8, 10) through the IFN-γR–mediated signaling pathway (13). Binding of IFN-γ to IFN-γR, which is ubiquitously but not uniformly expressed on all human nucleated cells (14), leads to transphosphorylation of IFN-γR–associated Janus-activated kinase kinases followed by phosphorylation and dimerization of cytosolic STAT1. The phosphorylated STAT1 (pSTAT1) is translocated to the nucleus as an active transcription factor (15-17) and binds to the IFN-γ activation site (GAS) element to activate transcription of the primary IFN-γ response genes (13, 18). Our previous studies showed that human colon carcinoma cells silence IRF8 expression through the IRF8 promoter DNA methylation (3). However, the molecular mechanisms underlying methylation-dependent inhibition of IRF8 activation by IFN-γ are unclear. In the present studies, we carried out detailed analysis of the molecular interactions between the IRF8 promoter DNA and IFN-γ–activated pSTAT1 in human colon carcinoma cells.

Results

IRF8 Protein Level Is Inversely Correlated with the Metastatic Phenotype In vivo

Six pairs of human primary colon carcinoma and lymph node metastases derived from six colon cancer patients were analyzed for IRF8 protein. IRF8 protein level and expression patterns were dramatically different between patients and between primary and metastatic tumors. In one patient, the primary tumor and lymph node metastases exhibited strong nuclear IRF8 staining and weak cytoplasmic IRF8 staining (Fig. 1A, *a1* and *b1*), whereas in two patients, strong cytoplasmic but no nuclear IRF8 staining was observed in both primary tumors and lymph node metastases (Fig. 1A, *a2* and *b2*; data not shown). In an additional two patients, strong nuclear but weak cytoplasmic IRF8 immunoreactivity was detected in primary tumors and only weak cytoplasmic staining but no nuclear staining was observed in the lymph node metastases (Fig. 1A, *a3* and *b3*; data not shown). The IRF8-specific staining level was moderate in the nuclei and weak in the cytoplasm of the primary tumor in patient 6, and IRF8 is undetectable in the lymph node metastases (Fig. 1A, *a4* and *b4*). As a positive control, we also stained human tonsil tissues for IRF8 protein under the same conditions and observed that IRF8 protein is only present in the nucleus (data not shown). Moreover, although IRF8 protein was detected in both nucleus and cytoplasm of the colon carcinoma cells, IRF8-specific staining was only observed in the nuclei of lymphocytes in the tumor-bearing lymph node (Fig. 1A, *b1-b3*). IRF8 is a transcription factor and is located in the nuclei of lymphocytes, and the nature of the cytoplasmic IRF8 staining in human colon carcinoma cells remains to be determined. IRF8 protein was not uniformly expressed in all tumor cells in the primary tumors; rather, IRF8-positive tumor cells are scattered in the tumor tissue.

To extend the above findings to a larger pool of human colorectal cancer specimens, we analyzed IRF8 protein levels in human colorectal carcinomas printed on tissue microarray. Among the 37 primary colorectal carcinoma tissues interpretable, 31 (84%) exhibited IRF8 protein staining in the nucleus (Fig. 1B, *a*). We also separately analyzed liver metastases derived from seven colorectal cancer patients. IRF8 protein was not detected in the nucleus of the tumor cells in five of the seven specimens (Fig. 1B, *b*). However, IRF8 protein was detected in the nucleus of the tumor cells in two of the seven (29%) liver metastases specimens (data not shown). Taken together, nuclear IRF8 protein is present in 81% (35 of 43) of primary colorectal carcinoma specimens and in 23% (3 of 13) of metastatic tumor specimens derived from colorectal cancer patients, respectively.

The IRF8 Promoter Region Is Frequently Methylated in Human Colorectal Carcinoma In vivo

To determine whether the IRF8 promoter is hypermethylated in human colorectal carcinoma under physiologic conditions, we isolated genomic DNA from 21 primary tumor specimens derived from 21 human colorectal cancer patients and liver metastases specimens derived from another 12 human colorectal cancer patients. Methylation-sensitive PCR (MS-PCR) analysis revealed that the IRF8 promoter is methylated in 43% (9 of 21) primary colon carcinoma specimens and in 83% (10 of 12) liver metastases specimens, respectively (Fig. 1C and D).

DNMT1 and DNMT3b Cooperate to Mediate the IRF8 Promoter DNA Methylation

We next made use of existing DNMT knockout cell lines (19) to determine which DNMT is responsible for the IRF8 promoter methylation. HCT116 is a colon carcinoma cell line isolated from poorly differentiated colon carcinoma and has been experimentally shown to be highly invasive (20). Reverse transcription-PCR (RT-PCR) analysis indicated that IRF8 is not detectable in HCT116 cells, and HCT116 cells did not respond to IFN-γ stimulation to activate IRF8 expression. Knocking down DNMT1 or DNMT3b alone did not result in constitutive or IFN-γ–induced IRF8 expression. However, knocking down both DNMT1 and DNMT3b rendered HCT116 cells responsive to IFN-γ to induce IRF8 expression in HCT116 cells (Fig. 2A). Next, HCT116 cells were treated with 5-azacytidine. Although 5-azacytidine did not result in constitutive IRF8 expression, demethylation rendered HCT116 cells susceptible to IFN-γ stimulation to express IRF8 (Fig. 2B). Overall, our results indicate that IFN-γ–regulated IRF8 activation is

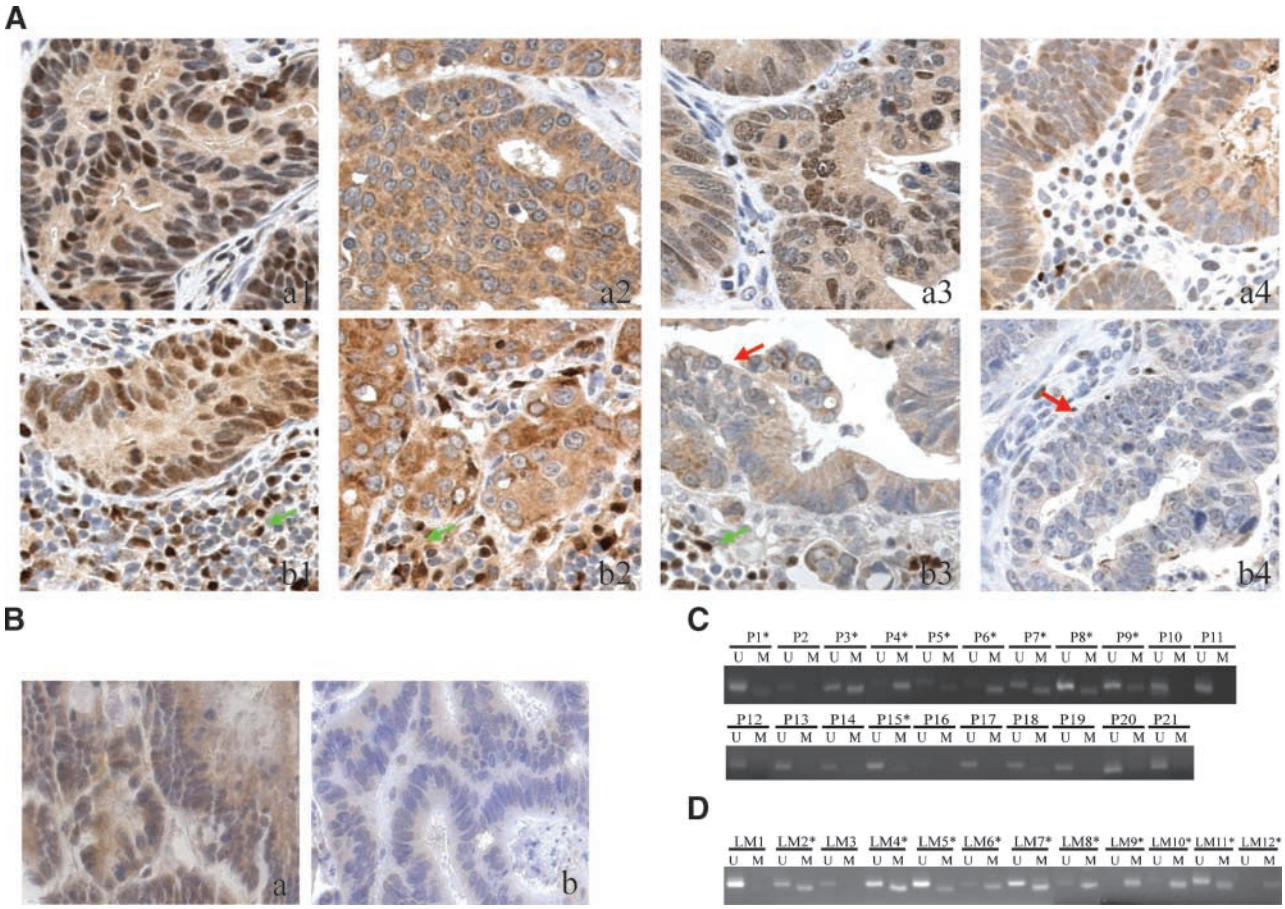

FIGURE 1. IRF8 protein level is inversely correlated with the methylation status of the IRF8 promoter in human colorectal carcinoma *in vivo*. **A.** Paraffin-embedded tissue sections were prepared from matched pairs of human primary colon carcinoma and lymph node metastases of six colon cancer patients and examined by immunohistochemistry with IRF8-specific antibody. Anti-IRF8 immunoreactivity is shown as the brown-stained areas; areas that were unreactive with the anti-IRF8 antibody are indicated by the blue (hematoxylin) counterstain. Staining of matched primary colon carcinoma tissue (*a1-a4*) and metastases-bearing lymph node (*b1-b4*) from four patients is shown. Red arrows, tumor nodules; green arrows, lymphocytes in the lymph node. **B.** Tissue microarray slides containing paraffin-embedded colorectal carcinoma and slides containing individual paraffin-embedded liver metastases tissue sections were also stained for IRF8 protein. Shown are representative images of IRF8 staining in primary colon carcinoma (*a*) and liver metastases (*b*). **C** and **D.** Methylation status of the IRF8 promoter in primary and metastatic human colorectal cancer specimens. Genomic DNA was extracted from frozen primary colon carcinoma specimens derived from 21 colorectal cancer patients (**C**, P1-P21), frozen liver metastases specimens (**D**, LM1-LM8), and paraffin-embedded liver metastases specimens (**D**, LM9-LM12) derived from another 12 human colorectal cancer patients. The genomic DNA was modified with sodium bisulfite as described in Materials and Methods and analyzed by MS-PCR using unmethylation (*U*) and methylation (*M*) primers. *, tumor specimens with methylated IRF8 promoter.

repressed by DNA methylation, and DNMT1 and DNMT3b cooperate to mediate methylation-dependent IRF8 transcriptional repression.

Epigenetically mediated transcriptional silencing events are often associated with gene promoter methylation, particularly at the CpG island (21-27). MS-PCR analysis indicated that the IRF8 promoter is indeed methylated in HCT116 cells. Knocking down DNMT1 or DNMT3b alone only resulted in minimal demethylation of the IRF8 promoter region. In contrast, knocking down both DNMT1 and DNMT3b completely demethylated the IRF8 promoter region (Fig. 2C), suggesting that DNMT1 and DNMT3b cooperate to methylate the IRF8 promoter. The IRF8 promoter region from +371 to −817 relative to the IRF8 transcription initiation site contains 108 CpG dinucleotides and 262 non-CpG cytosines. Bisulfite DNA sequencing revealed that all cytosines of the 108 CpG dinucleotides were methylated, whereas none of the 262 non-CpG cytosines was methylated (Fig. 2D). To further analyze the degree of DNA methylation, we amplified the IRF8 promoter DNA fragment from −174 to −585 relative to the IRF8 transcription initiation site from bisulfite-treated genomic DNA and cloned the amplified DNA fragment to pCR2.1 vector. Three individual clones were sequenced. There are 45 CpG dinucleotides in this region and 43 CpGs were methylated in two clones and 42 CpGs were methylated in the third clones (Fig. 2D).

DNA Methylation Does Not Inhibit pSTAT1 Binding to the GAS Element of the IRF8 Promoter

Next, we sought to determine whether methylation inhibits pSTAT1 binding to the IRF8 promoter in HCT116 cells. We first analyzed induction of STAT1 phosphorylation by IFN-γ.

Western blotting analysis indicated that STAT1 is phosphorylated in HCT116 and sublines after IFN-γ treatment (Fig. 3A), suggesting that lack of IRF8 up-regulation by IFN-γ is not due to lack of STAT1 activation in the colon carcinoma cells. We next did electrophoretic mobility shift assay (EMSA). Incubation of the 107-bp IRF8 promoter DNA probe with nuclear extracts prepared from IFN-γ–treated SW480 and HCT116 cells indicated that pSTAT1 binds to the GAS-containing DNA fragment *in vitro* (Fig. 3B). Next, SW480, HCT116, and HCT116.DKO cells were cultured in the presence of IFN-γ for 1 hour and used for chromatin immunoprecipitation (ChIP) assay using pSTAT1-specific monoclonal antibody. PCR amplification of the IP with IRF8 promoter-specific primers that flank the GAS element revealed that STAT1 is associated with the IRF8 promoter in IFN-γ–treated SW480 and HCT116.DKO cells (Fig. 3C). However, STAT1 binding to the IRF8 promoter was also detected in IFN-γ–treated HCT116 (Fig. 3C).

The above ChIP assays indicated that pSTAT1 is associated with the methylated IRF8 promoter region *in vivo*. However, it does not rule out the possibility that IRF8 is associated with the IRF8 promoter through another protein [i.e., methyl-CpG binding domain proteins (MBD)] but does not directly bind to the GAS site in the methylated IRF8 promoter region. The consensus GAS element has a characteristic dyad symmetry consisting of an inverted GAA repeats separated by three nucleotides (*TTC*NNG*GAA*; Fig. 4A). Our bisulfite DNA sequencing revealed that the cytosine in the *TTC* sequence is not methylated; however, the cytosine of the CpG between the two inverted repeats is methylated (Fig. 4A). Therefore, the GAS element in the human IRF8 promoter might be epigenetically "mutated" in human colon carcinoma cells. To

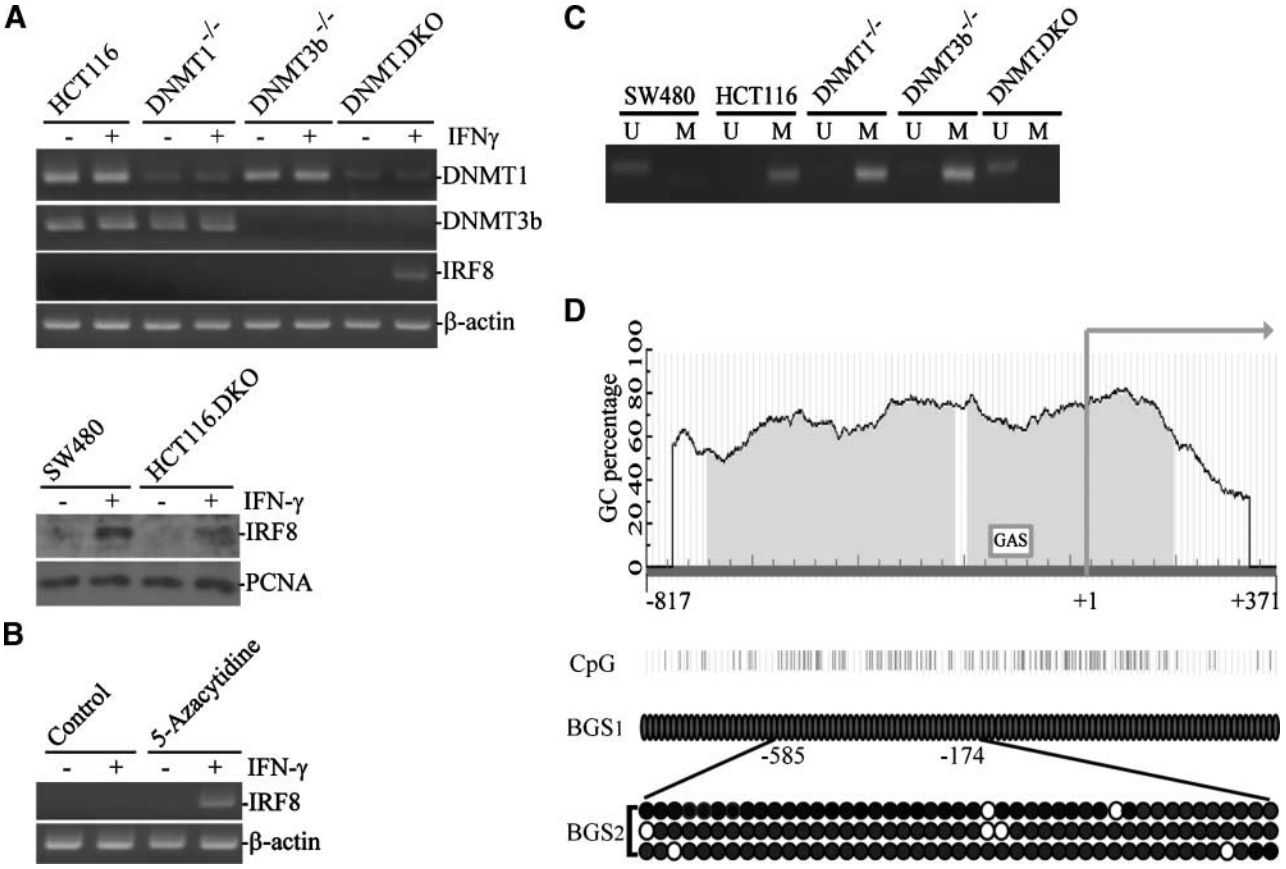

FIGURE 2. DNMT1 and DNMT3b cooperate to methylate IRF8 promoter and repress IRF8 expression. **A.** Analysis of DNMT1, DNMT3b, and IRF8 expression levels. HCT116 and DNMT knockout sublines were either not treated or treated with IFN-γ for ~24 h and then analyzed for IRF8 transcript levels. β-Actin was used as a normalization standard. Bottom, Western blotting analysis of IRF8 protein level. SW480 and HCT116.DKO cells were treated as in **A**. Nuclear extracts were prepared from the tumor cells and analyzed for IRF8 protein level. Proliferating cell nuclear antigen (*PCNA*) was used as normalization standard. **B.** Demethylation treatment restored HCT116 cells to IRF8 induction by IFN-γ. HCT116 cells were either not treated or treated with 5-azacytidine as described in Materials and Methods. The treated cells were cultured in the presence or absence of IFN-γ for ~24 h and then used for RT-PCR analysis of IRF8 expression level. β-Actin was used as a normalization standard. **C.** MS-PCR analysis of the IRF8 promoter region. U, unmethylated; M, methylated. **D.** DNA sequencing of bisulfite-modified genomic DNA isolated from HCT116 cells. Top, CpG island as predicted by computer program MethPrimer (Chemicon). The vertical bar (CpG as indicated at the *left*) at the bottom of the CpG island diagram indicates locations of CpG dinucleotides. The nucleotide positions relative to the IRF8 transcription initiation site (+1) are indicated by numbers. The CpG island is shown as light shaded area. The GAS element is indicated by a box. A 1,188-bp IRF8 promoter DNA region (+371 to −817 relative to the IRF8 transcription initiation site) containing the entire CpG island was amplified by PCR from bisulfite-modified HCT116 cell genomic DNA and the PCR products were directly sequenced (*BSG1*). Shown is the methylation status of CpGs. Filled circles, methylated CpGs. Part of the 1,188-bp IRF8 promoter region (−174 to −585) was also amplified by PCR and cloned to pCR2.1 vector. Three individual clones were sequenced and the methylation status of these three clones is shown (*BGS2*). Filled circles, methylated CpGs; open circles, unmethylated CpGs.

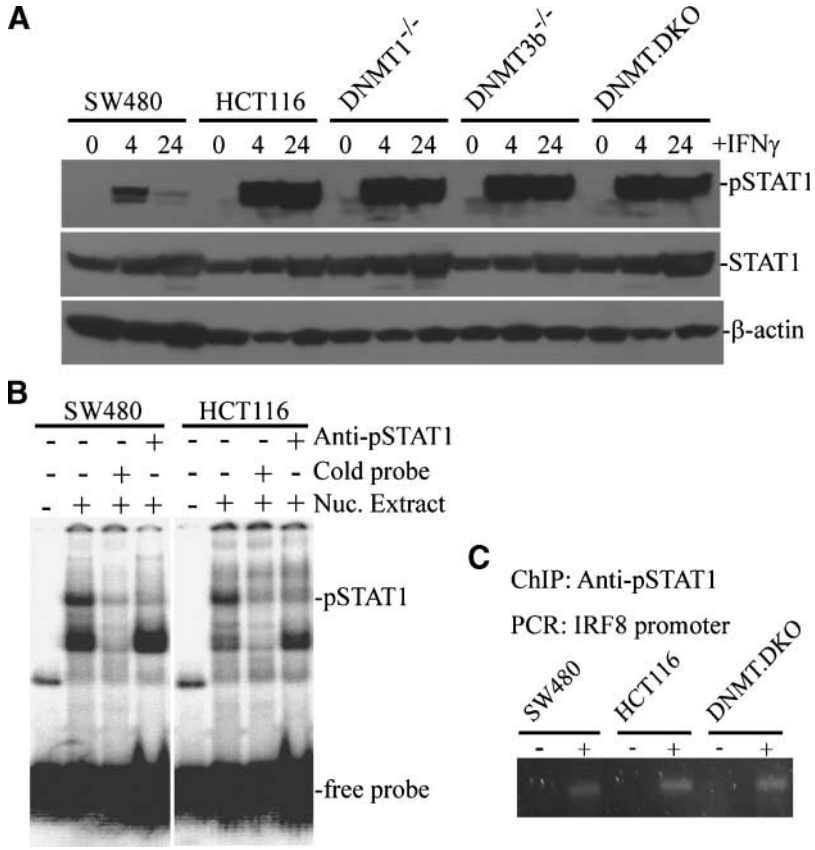

FIGURE 3. IRF8 promoter methylation has no direct effect on pSTAT1 association with the IRF8 promoter. **A.** Western blot images of pSTAT1 and STAT1 in human colon carcinoma cell lines/sublines. Tumor cells were treated with IFN-γ for 4 and 24 h, respectively, and analyzed by Western blotting. β-Actin was used as normalization control. **B.** EMSA of pSTAT1 binding to the IRF8 promoter *in vitro*. The 107-bp GAS-containing IRF8 promoter DNA fragment was incubated with nuclear extracts (+) prepared from IFN-γ–treated SW480 and HCT116 cells, respectively, and analyzed by gel electrophoresis. Cold probe and anti-pSTAT1 monoclonal antibody were included as specificity controls as described in Materials and Methods. **C.** ChIP analysis of pSTAT1 association with the IRF8 promoter in the indicated cell lines/sublines. The ChIP was carried out with anti-pSTAT1 monoclonal antibody (+), whereas the reaction with no antibody (–) was used as negative controls.

determine whether this "epigenetic mutation" within the GAS element directly inhibits pSTAT1 binding to the GAS element-containing DNA, The C nucleotide of the CpG between the inverted GAA repeat (*TTC*T*C*G*GAA*) was mutated to a T (*TTC*T*T*G*GAA*) in the DNA probe. Mutation of the C to a T mimics methylation of the cytosine nucleotide. The prediction is that if methylation of this C inhibits pSTAT1 binding to the GAS element, then pSTAT1 in the nuclear extract should not bind to the mutated probe. Our EMSA data showed that mutation of this cytosine does not inhibit pSTAT1 binding to the GAS DNA element (Fig. 4A).

To further determine whether DNA methylation in the region adjacent to the GAS element directly inhibit pSTAT1 binding to the IRF8 promoter DNA, we methylated the 107-bp IRF8 promoter DNA probe with CpG methylase M.*Sss*I *in vitro* and used the methylated DNA probe in EMSA. As a quality control, we analyzed the methylated DNA probe with *Nci*I restriction endonuclease. *Nci*I cleaves at a consensus sequence CCSGG and its activity is impaired by DNA methylation at sites with overlapping CpG. The 107-bp IRF8 promoter DNA fragment contains two *Nci*I cleavage sites (CCGGG and CCCGG). DNA methylation should impair *Nci*I activity to cleave the CCGGG sequence but not the CCCGG sequence. The control probe (treated with *Nci*I buffer and *S*-adenosylmethionine but not M.*Sss*I) was efficiently cleaved into small fragments and the M.*Sss*I-treated DNA probe exhibited significantly increased resistance to *Nci*I cleavage (Fig. 4B), indicating that the DNA probe is methylated by M.*Sss*I. Next, the methylated DNA probe was incubated with nuclear extracts prepared from IFN-γ–treated HCT116 cells and analyzed by EMSA. As shown in Fig. 4B, pSTAT1 was detected to bind to the methylated IRF8 promoter DNA. The pSTAT1 binding was displaced by anti-pSTAT1 antibody and cold probe but not by IgG control and the 102-bp cold probe with mutation of the GAS consensus sequence (Fig. 4B), suggesting that pSTAT1 specifically binds to the GAS element of the methylated IRF8 promoter DNA. To further validate the pSTAT1 binding specificity to the GAS sequence, we synthesized short oligonucleotides of both strands of the human IRF8 GAS element and annealed the oligonucleotides to form dsDNA. We made a 24-bp wild-type (wt) GAS DNA probe and a 21-bp mutant GAS DNA probe. EMSA analysis indicated that incubation of nuclear extracts prepared from IFN-γ–treated HCT116 cells with the 24-bp GAS DNA probe resulted in two protein-DNA complexes (Fig. 4C, *lane 2*). Anti-pSTAT1 antibody displaced the upper band, but incubation with IgG control did not affect the protein-DNA complex formation (Fig. 4C, *lane 3* and *4*). Addition of excess amount of unlabeled probe competed away both DNA-protein complexes. However, addition of excess amount of the unlabeled 21-bp mutant GAS DNA probe only competed away the lower band (Fig. 4C, *lanes 5* and *6*). Therefore, the upper band is the pSTAT1 and GAS DNA complex. Taken together, our data strongly suggest that IFN-γ–activated pSTAT1 specifically binds to the GAS element of the IRF8 promoter and DNA methylation in the IRF8 promoter region does not inhibit

pSTAT1 binding to the IRF8 promoter DNA in human colon carcinoma cells.

DNA Methylation Inhibited STAT1 Function in the IRF8 Promoter

Our EMSA assays indicated that pSTAT1 can bind to the IRF8 promoter *in vitro* and our ChIP assays revealed that pSTAT1 is associated with the IRF8 promoter *in vivo* regardless of the methylation status of the IRF8 promoter. Thus, our data suggest that DNA methylation neither directly inhibits pSTAT1 binding to the GAS element of the IRF8 promoter nor secondarily blocks pSTAT1 association with the IRF8 promoter. Because pSTAT1 does not activate IRF8 expression in the tumor cells with methylated IRF8 promoter, we hypothesize that the IRF8 promoter methylation might lead to binding of MBD proteins that recruit repressors to inhibit pSTAT1 function. Therefore, although pSTAT1 is associated with the IRF8 promoter region, its function is inhibited (28). In the literature, it has been shown that protein inhibitor of activated STAT1 (PIAS1) is a potent pSTAT1 inhibitor. PIAS1 protein directly binds to pSTAT1 to inhibit pSTAT1-mediated gene activation (29-31). It has also been shown that PIAS1 can sumoylate MBD1 (31, 32), suggesting that PIAS1 might form a complex with MBD1. RT-PCR and Western blotting analysis revealed that MBD1 and PIAS1 mRNA and proteins are expressed in both SW480 and HCT116 cells (Fig. 5A and B). We used MBD1-specific antibody to immunoprecipitate the MBD1 protein complexes from IFN-γ–treated SW480 and HCT116 cells and then examined the association of PIAS1 and pSTAT1 with MBD1. Western blotting analysis revealed that PIAS1 is associated with MBD1 in both SW480 and HCT116 cells. pSTAT1 is also associated with MBD1. Interestingly, ~10.4 times more pSTAT1 is associated with the PIAS1/MBD1 protein complex in HCT116 cells than in SW480 cells (Fig. 5C). Because pSTAT1 is associated with the IRF8 promoter (Fig. 3C), our data thus suggest that pSTAT1 is preferentially associated with the PIAS1/MBD1 protein complex at the methylated IRF8 promoter region.

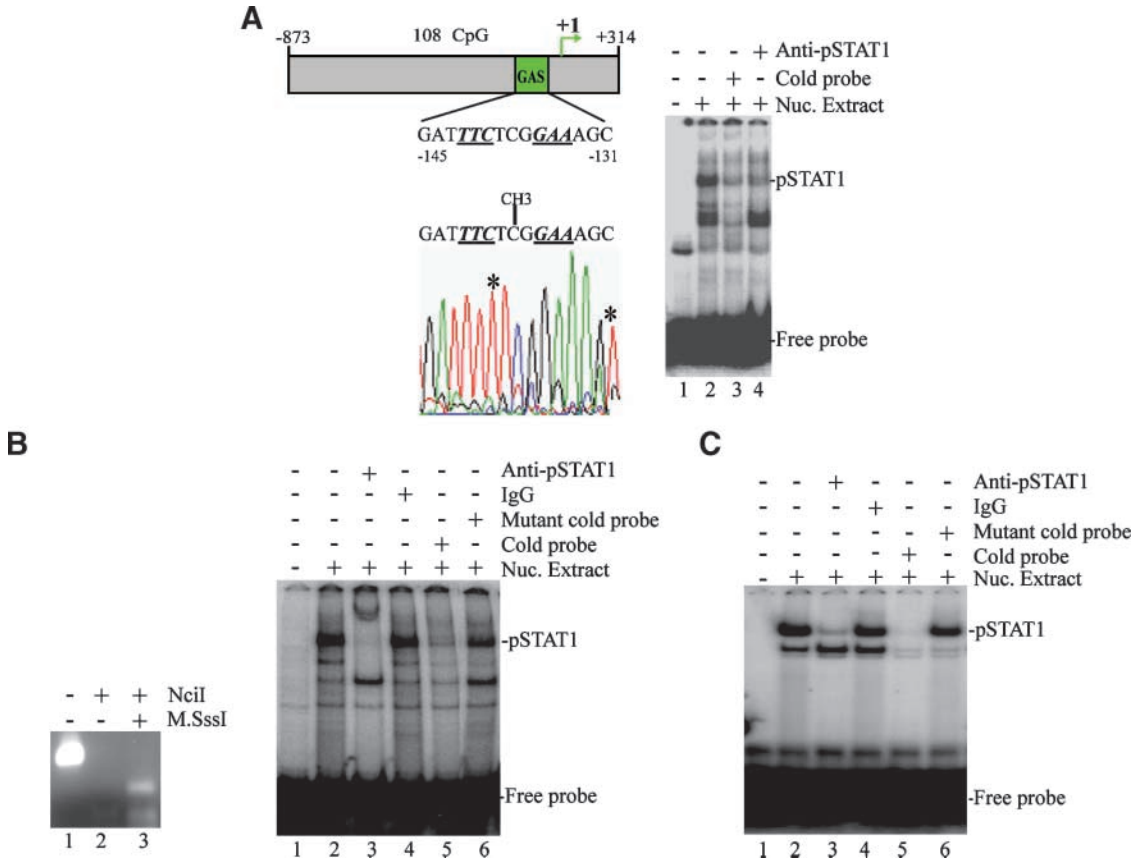

FIGURE 4. Methylation does not affect pSTAT1 binding to the IRF8 promoter. **A.** Genomic DNA isolated from HCT116 cells was bisulfite treated and sequenced. Top, location of the GAS element; bottom, methylation of cytosine within the GAS element. *, bisulfite conversion of unmethylated C to T. Left, methylated C is indicated with "CH3-C"; right, EMSA of pSTAT1 binding to mutated GAS element. The C nucleotide of the CpG between the inverted GAA repeat (*TTCTCGGAA*) was mutated to a T (*TTCTTGGAA*) in the 107-bp IRF8 promoter DNA probe. The probe/pSTAT1 complex is indicated at the right. **B.** EMSA of pSTAT1 and *in vitro* methylated IRF8 promoter DNA probe. The 107-bp DNA probe was methylated with M.*Sss*I *in vitro* as described in Materials and Methods. Left, methylation status of the DNA probe is verified by methylation-sensitive restriction endonuclease *Nci*I. Lane 1, unmethylated input DNA; lane 2, unmethylated DNA probe digested with *Nci*I; lane 3, M.*Sss*I-methylated DNA probe digested with *Nci*I. Right, the methylated 107-bp DNA probe was incubated with nuclear extracts isolated from IFN-γ–treated HCT116 cells in the absence (*lane 2*) and presence of anti-pSTAT1 antibody (*lane 3*), IgG control (*lane 4*), the 107-bp cold probe (*lane 5*), or the 102-bp cold mutant DNA probe (*lane 6*). Right, pSTAT1-DNA complex. **C.** EMSA of pSTAT1 and GAS DNA element. The 24-bp DNA probe containing the GAS consensus sequence was incubated with nuclear extracts isolated from IFN-γ–treated HCT116 cells in the absence (*lane 2*) and presence of anti-pSTAT1 antibody (*lane 3*), IgG control (*lane 4*), the 24-bp cold probe (*lane 5*), or the 21-bp cold mutant DNA probe (*lane 6*). Right, pSTAT1-DNA complex.

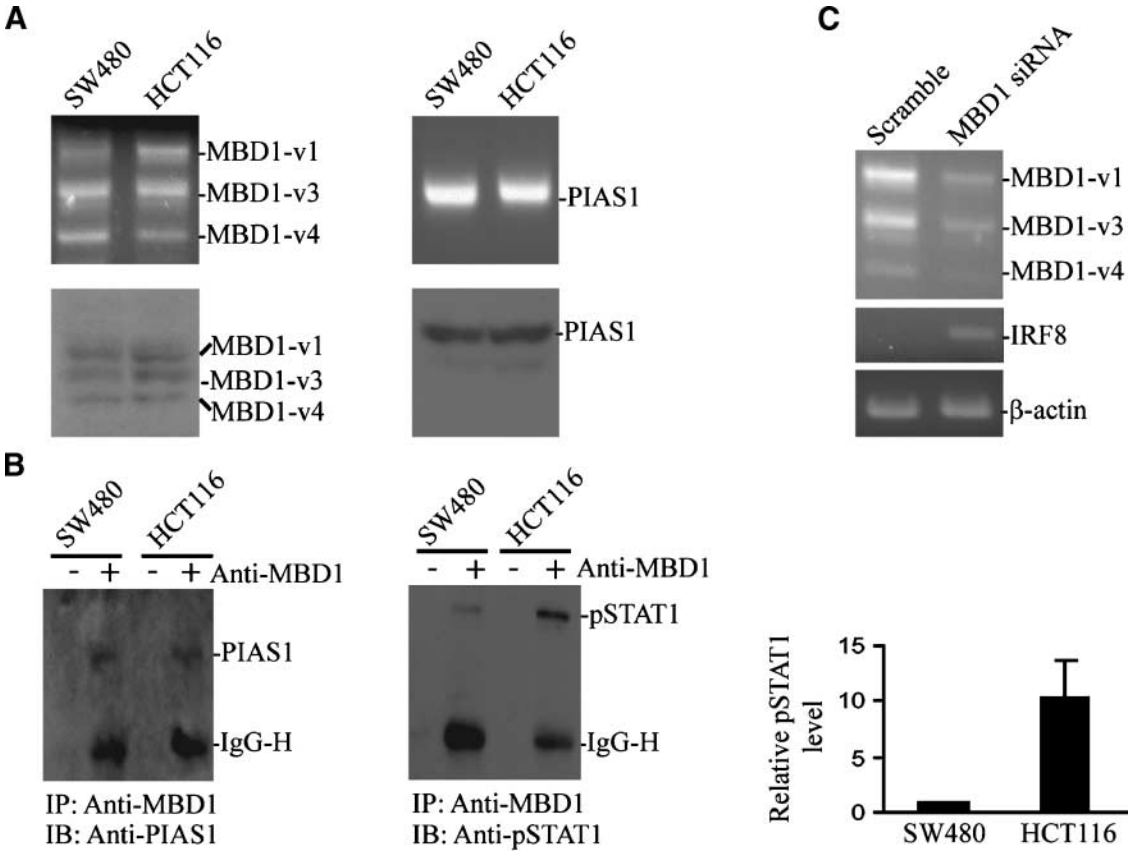

FIGURE 5. MBD1 recruits PIAS1 to inhibit pSTAT1 function at the methylated IRF8 promoter region. **A.** RT-PCR and Western blotting analysis of MBD1 and PIAS in SW480 and HCT116 cells. MBD1 has five known isoforms. Left, MBD1 variants 1, 3, and 4 were detected and indicated. Top, transcript levels; bottom, protein level. **B.** IP-Western analysis of association of PIAS1 and pSTAT1 with MBD1 protein. SW480 and HCT116 cells were treated with IFN-γ for 1 h and cell lysates were prepared for immunoprecipitation of MBD1 proteins using MBD1-specific antibody. The IPs were blotted and probed with anti-PIAS (*left*) or anti-pSTAT1 (*middle*) antibody. PIAS1, pSTAT1, and the heavy chain of the antibody (*IgG-H*) are indicated. Control lanes (−) show immunoprecipitation using protein A beads alone (no MBD1 antibody). The pSTAT1 level shown in the right panel is quantified by measuring the band intensity using NIH ImageJ program. The relative level of MBD1/PIAS1-associated pSTAT1 in SW480 cells is normalized based on IgG-H intensity and arbitrarily set at 1. Right, the MBD1/PIAS1-associated pSTAT1 level in HCT116 cells is presented as fold of that in SW480 cells. **C.** Silencing MBD1 expression leads to IRF8 activation by IFN-γ in HCT116 cells. HCT116 cells were transiently transfected with scramble siRNA or human MBD1-specific siRNA followed by treatment with IFN-γ. The cells were analyzed by RT-PCR for MBD1 and IRF8 expression level. β-Actin was used as normalization standard.

To validate the function of MBD1 in methylation-dependent IRF8 repression in human colon carcinoma cells, we used human MBD1-specific small interfering RNA (siRNA) to silence MBD1 expression in HCT116 cells and analyzed the effects of loss of MBD1 expression on IFN-γ–induced IRF8 activation. We tested four MBD1-specific siRNAs that target the conserved regions of all known MBD1 variants and observed that one siRNA (Hs_MBD1_9) knocked down the expression level of MBD1 variants 1, 3, and 4 by approximately 70% to 77% in HCT116 cells (Fig. 5C). Silencing MBD1 expression resulted in activation of IRF8 by IFN-γ in HCT116 cells (Fig. 5C). Taken together, our data indicate that MBD1 is responsible, at least in part, for the methylation-dependent IRF8 repression in human colon carcinoma cells.

Discussion

Gene expression is frequently regulated by epigenetic events in tumor cells (27, 33-38). It is apparent that loss of IRF8 expression in human colorectal carcinoma cells is mediated, at least in part, by IRF8 promoter DNA methylation (Figs. 1 and 2). DNA methylation is mediated by DNMTs, and five DNMTs (DNMT1, DNMT2, DNMT3a, DNMT3b, and DNMT3L) have been identified in mammalian cells (39). In this study, we showed that DNMT1 and DNMT3b cooperate to methylate the IRF8 promoter. Knocking down DNMT1 or DNMT3b alone only resulted in minimal demethylation of the IRF8 promoter region (Fig. 2), suggesting that DNMT1 and DNMT3b cooperatively methylate the IRF8 promoter. It seems that IRF8 promoter is methylated not only in metastatic colorectal carcinoma but also in the primary colon carcinoma. In a previous study, we showed that metastatic tumor cell subsets preexist in the primary tumor population (40). It has also been shown that the poorly differentiated primary human colon carcinoma cells are highly invasive *in vivo*, whereas the well-differentiated tumor cells were not invasive (41-43). In the present study, we observed that IRF8 promoter is methylated in ~43% of the primary colorectal carcinoma tumors. Therefore, it is possible that these primary colon carcinoma cells with

methylated IRF8 promoter might be the metastatic progenitor cells within the primary tumor population. Actually, we have observed that the IRF8 promoter is also methylated in another poorly differentiated and invasive primary colon carcinoma cell line RKO (44) that expresses no detectable IRF8 (data not shown). However, the links between the IRF8 promoter hypermethylation and metastatic capability of these putative metastatic progenitor cells in the primary tumor population remain to be determined.

IFN-γ up-regulates IRF8 expression through activation of STAT1 in the IFN-γR signaling pathway. The activated STAT1 binds to the GAS element in the IRF8 promoter and activates IRF8 transcription (13). In this study, we showed that STAT1 is activated in the IRF8-refractory colon carcinoma cell line (Fig. 3A); however, activation of STAT1 did not lead to IRF8 activation (Fig. 2A). Two models have been proposed to explain the effects of promoter DNA methylation on gene silencing (44-46). The first model postulates that DNA methylation represents an epigenetic mutation of the transcription factor binding site and thus directly inhibits the transcription factor binding to the promoter to activate transcription (44). The second model proposes that the methylated promoter DNA recruits MBD proteins to the promoter and secondarily blocks transcription factor binding (45, 47). In this study, the STAT1 binding consensus sequence GAS is located in the methylated CpG island of the IRF8 promoter and the cytosine of a CpG dinucleotide within the GAS element is methylated (Fig. 4A). However, our EMSA data indicated that methylation of this cytosine and cytosines of the CpG dinucleotides adjacent to the GAS element does not inhibit pSTAT1 binding to the GAS element *in vitro* (Fig. 4). Our ChIP assay revealed that pSTAT1 can associate with the GAS region of the IRF8 promoter *in vivo* regardless of the methylation status of the IRF8 promoter region. Thus, DNA methylation neither directly inhibits pSTAT1 binding to the GAS element of the IRF8 promoter nor secondarily blocks the association of pSTAT1 with the IRF8 promoter, suggesting a methylation-dependent novel mechanism that inhibits IRF8 activation by pSTAT1 at methylated IRF8 promoter site.

PIAS1 is a potent pSTAT1 inhibitor and can directly bind to pSTAT1 to inhibit pSTAT1-mediated gene activation (29-31). The fact that PIAS1 can sumoylate MBD1, a methyl-DNA binding protein (31, 32), suggests that PIAS1 might form a complex with MBD1 in human colon carcinoma cells and thus associates with the methylated IRF8 promoter region. Our IP-Western analysis revealed that both PIAS1 and pSTAT1 proteins form complexes with MBD1 in SW480 and HCT116 cells. Interestingly, much more pSTAT1 is associated with MBD1 in HCT116 cells than in SW480 cells (Fig. 5B), suggesting that DNA methylation might preferentially enhance MBD1 association with pSTAT1 and thereby bring PIAS1 to the pSTAT1 protein complex. Because PIAS1 is a potent inhibitor of pSTAT1 (29-31), contact between PIAS1 and pSTAT1 would effectively inhibit pSTAT1 function, although pSTAT1 is associated with the GAS element in the methylated IRF8 promoter. However, although we have determined that MBD1 is responsible, at least in part, for methylation-dependent IRF8 repression in human colon carcinoma cells (Fig. 5C), initial attempts using ChIP technique have failed to detect MBD1 and PIAS1 association with the IRF8 promoter in SW480 and HCT116 cells *in vivo*. Further studies are needed to elucidate the precise molecular mechanism underlying methylation-dependent interactions between pSTAT1, MBD1, PIAS1, and the IRF8 promoter in human colon carcinoma cells.

Materials and Methods

Cell Lines and Tumor Tissues

The following cell lines were provided by Dr. B. Vogelstein (Johns Hopkins University, Baltimore, MD) through Dr. M. Thangaraju (Medical College of Georgia, Augusta, GA): human colon carcinoma cell line HCT116, DNMT1 knockout HCT116 (HCT116.DNMT1$^{-/-}$), DNMT3b knockout (HCT116.DNMT3b$^{-/-}$), and DNMT1/DNMT3b double knockout (HCT116.DKO) cells. Human tumor tissues were excised from freshly resected surgical specimens at Medical College of Georgia Medical Center and Charite, Berlin. For immunohistochemical staining of IRF8 protein, tissues were fixed with formalin and embedded in paraffin. For genomic DNA isolation, portions of the tissues were excised to isolate genomic DNA using DNeasy Tissue kit (Qiagen) according to the manufacturer's instructions. All experiments involving human tissues were conducted in accordance with protocols approved by the institutional review board.

Immunohistochemistry

Tissue sections were cut from formalin-fixed, paraffin-embedded tissue blocks. Specimens were blocked with normal goat serum (1.5%) and then incubated with a goat anti-IRF8 polyclonal antibody (Santa Cruz Biotechnology) at 1:50 to 1:100 dilution for 30 min followed by rinsing and staining with anti-goat biotinylated antibody (1:2,000) for another 30 min. Binding was visualized by incubation with 3,3′-diaminobenzidine solution (Sigma) followed by rinsing and counterstaining with hematoxylin. Positive and negative controls were done in parallel. Each section was also stained with H&E to localize the tumors in the tissues.

RT-PCR Analysis

Total RNA was isolated from cells using Trizol (Invitrogen) according to the manufacturer's instructions and was used for first-strand cDNA synthesis using the ThermoScript RT-PCR system (Invitrogen). The cDNA was then used as template for PCR amplification of the indicated transcripts as previously described (48, 49). The PCR primer sequences are as follows: IRF8, 5′-CCAGATTTTGAGGAAGTGACGGAC-3′ (forward) and 5′-TGGGAGAATGCTGAATGGTGC-3′ (reverse); DNMT1, 5′-CGTGGAGTATGGGGAGGACC-3′ (forward) and 5′-ATCTCTGGCTCGCTCGGCTCACAG-3′ (reverse); DNMT3b, 5′-CCAACAACAAGAGCAGCCTGG-3′ (forward) and 5′-GCACTCCACACAGAAACACCG-3′ (reverse); β-actin, 5′-ATTGTTACCAACTGGGACGACATG-3′ (forward) and 5′-CTTCATGAGGTAGTCTGTCAGGTC-3′ (reverse); MBD1, 5′-ACCACCCCCATCACAGTCCC-3′ (forward) and 5′-TGGAGGCAGAATCATCCTTGTTC-3′ (reverse); and PIAS1, 5′-CATTGGAGCATCAGGTAGCGTC-3′ (forward) and 5′-CGGCAAGCAAGGAGGTGTTG-3′ (reverse). The PCR cycle

number was 30 for IRF8, DNMT1, DNMT3b, MBD1, and PIAS1 and 23 for β-actin.

Cell Treatment

For demethylation treatment with 5-azacytidine, cells were treated for 24 h on days 2 and 5 with 5-azacytidine (Sigma) at a final concentration of 1 μg/mL. After the second treatment (i.e., on day 6), medium was changed and recombinant human IFN-γ (R&D Systems) was added to the culture to a final concentration of 250 units/mL. Twenty-four hours later, cells were harvested for analysis for IRF8 expression.

Sodium Bisulfite Treatment and MS-PCR Analysis

Genomic DNA was purified using DNeasy Tissue kit (Qiagen) according to the manufacturer's instructions. Extraction of genomic DNA from paraffin-embedded tissues was carried out as previously described (35). Sodium bisulfite treatment of genomic DNA was carried out using CpGenome Universal DNA Modification kit (Chemicon) according to the manufacturer's instructions. MS-PCR was carried out as previously described (3).

Sodium Bisulfite Treatment and Genomic DNA Sequencing

The bisulfite-modified genomic DNA was used as template for PCR amplification of the human IRF8 promoter region. Eight PCR amplifications were carried out to amplify an 1,188-kb region of the IRF8 promoter. The amplified DNA fragments were directly sequenced from both directions using M13 forward or M13 reverse primers. The sequences were assembled using Sequencher v4.7 (SeqWright). A DNA fragment (−174 to −585 relative to IRF8 transcription initiation site) was also amplified from the modified genomic DNA and cloned to the pCR2.1 vector (Invitrogen). Three individual clones were sequenced.

ChIP Assay

ChIP assay was carried out according to protocols from Upstate Biotech. Immuoprecipitation was carried out using anti-pSTAT1 antibody (BD Biosciences) and agarose-protein A beads (Upstate). The protein-DNA complexes were eluted from beads and the cross-linking was reversed. The DNA was purified from the eluted solution and used for PCR with forward primer 5′-TGGACCCCAGGTGTGAGGAG-3′ and reverse primer 5′-CCGACCAATAGCGTCAGC-3′.

Western Blotting Analysis

Western blotting analysis was carried out as previously described (50). For total cell lysate preparation, tumor cells were lysed in lysis buffer containing 20 mmol/L HEPES (pH 7.4), 20 mmol/L NaCl, 10% glycerol, 1% Triton X-100, and protease and phosphatase inhibitor cocktails (Calbiochem). For nuclear extract preparation, tumor cells were resuspended in cytosol buffer [10 mmol/L HEPES (pH 7.0), 40 mmol/L KCl, 3 mmol/L $MgCl_2$, 5% glycerol, 0.2% NP40, and protease and phosphatase inhibitor cocktails] and centrifuged immediately for 2 min. The pellet was lysed in nuclei buffer [20 mmol/L HEPES (pH 7.9), 420 mmol/L KCl, 1.5 mmol/L $MgCl_2$, 0.5 mmol/L DTT, 0.2 mmol/L EDTA, 25% glycerol, and protease and phosphatase inhibitor cocktails] and incubated on ice for 30 min. Total cell lysate and nuclear extracts were separated by 4% to 20% SDS-PAGE gradient gels, transferred to Immobilon-P membranes (Millipore), and probed with primary antibodies. Anti-IRF8 antibody (C-19, Santa Cruz Biotechnology) was used at a 1:200 dilution, anti-pSTAT1 antibody at 1:1,500, anti-STAT1 (BD Biosciences) at 1:2,000, anti-MBD1 (Santa Cruz Biotechnology) at 1:300, anti-PIAS1 (Santa Cruz Biotechnology) at 1:1,000, anti-proliferating cell nuclear antigen (BD Biosciences) at 1:1,000, and anti-β-actin (Sigma) at 1:5,000. Bands were detected using the enhanced chemiluminescence Plus Western detection kit (Amersham Pharmacia Biotech).

Immunoprecipitation

Tumor cells were lysed in isotonic buffer [20 mmol/L HEPES (pH 7.4), 142.5 mmol/L KCl, 5 mmol/L $MgCl_2$, 1 mmol/L EDTA, and 0.2% NP40] plus protease and phosphatase inhibitor cocktails (Calbiochem) on ice for 1 h. The lysates were precleared with protein A agarose (Pierce) for 1 h at 4°C. The precleared lysates were incubated with anti-MBD1 antibody overnight at 4°C. Protein A agarose was then added to the lysate and incubated at 4°C for 1 h. The agarose beads were washed for 5 min at 4°C for three times. The bound proteins were eluted by resuspending the washed beads in SDS-protein gel loading buffer and heating at 100°C for 5 min. The eluted proteins were separated by 4% to 20% SDS-PAGE gradient gels, transferred to Immobilon-P membranes, and probed with primary antibodies. Anti-PIAS antibody (C-20, Santa Cruz Biotechnology) was used at a 1:300 dilution and anti-pSTAT1 antibody at 1:1,000. Bands were detected using the enhanced chemiluminescence Plus Western detection kit.

In vitro *Methylation of DNA Probe*

DNA fragment was incubated in the absence (control DNA probe) or presence of M.*Sss*I (New England Biolabs) at 37°C for 2 h. The reactions were stopped by incubation at 65°C for 20 min. The DNA was purified using the PCR purification kit (Qiagen). To verify the methylation of the purified DNA, the purified DNA was incubated with *Nci*I at 37°C for 2 h and analyzed by agarose gel electrophoresis.

Protein-DNA Binding Assay

Nuclear extracts were prepared from IFN-γ–treated tumor cells as described (51). Two groups of DNA probes were used in EMSA. The first group of probes is PCR-amplified DNA fragments. A 107-bp DNA fragment was amplified from SW480 genomic DNA. The probe contains the human GAS element. The primers are 5′-CCCCAGGTGTGAGGAGCG-3′ (forward) and 5′-AGTGCTCTGCTTTCCGAGAAATC-3′ (reverse). A mutant DNA probe was also amplified from SW480 genomic DNA. The forward primer is the same as the forward primer for the wt probe. The reverse primer is 5′-AGTGCTCTGCTTTCC*A*AGAAATC-3′. The point mutation is a C to T switch inside the GAS element. A second mutant DNA probe (102 bp) was also amplified from the genomic DNA. The forward primer is the same as the forward primer for the wt

probe. The reverse primer is 5′-TCTGCTTTCCGA*TCC*ATTCACT-3′. The conserved TTC sequence of the GAS element was converted to GGA in this mutant probe. The second group of probes is short DNA fragments prepared from synthesized oligonucleotides. The following oligonucleotides are synthesized: 5′-AGTGATTTCTCGGAAAGCAGAGCA-3′ (wt probe sense), 5′-TGCTCTGCTTTCCGAGAAATCACT-3′ (wt probe antisense), 5′-AGTGATGGATCGGAAAGCAGA-3′ (mutant probe sense), and 5′-TCTGCTTTCCGA*TCC*ATCACT-3′ (mutant probe antisense). The wt probe oligonucleotides were annealed to prepare a 24-bp dsDNA probe containing the wt GAS consensus sequence (AGTGAT*TTC*TCG*GAA*AGCACAGAGCA). The mutant probe oligonucleotides were annealed to form a 21-bp dsDNA probe containing a mutated GAS element with conversion of TTC to GGA (AGTGAT*GGA*TCG*GAA*AGCAGA). The probes were end labeled with [γ-^{32}P]ATP using T4 DNA polynucleotide kinase (Invitrogen) and purified with Micro Bio-Spin 30 column (Bio-Rad). The end-labeled probes (1 ng) were incubated with nuclear extracts (5 μg) in protein-DNA binding buffer [10 mmol/L Tris-HCl (pH 7.5), 1 mmol/L $MgCl_2$, 0.5 mmol/L EDTA, 0.5 mmol/L DTT, 50 mmol/L NaCl, 4% glycerol, and 0.05 mg/mL poly(deoxyinosinic-deoxycytidylic acid)·poly(deoxyinosinic-deoxycytidylic acid)] for 20 min at room temperature. For specificity controls, unlabeled probe was added to the reaction at a 1:100 molar excess. Anti-pSTAT1 monoclonal antibody (Santa Cruz Biotechnology) was also included to identify pSTAT1-specific DNA binding. Anti-pSTAT1 was incubated with the nuclear extracts for 30 min on ice before addition of labeled probes. DNA-protein complexes were separated by electrophoresis in 5% polyacrylamide gels in 45 mmol/L Tris borate and 1 mmol/L EDTA (pH 8.3). The gels were dried and exposed to a phosphoimage screen (Molecular Dynamics) and the images were acquired using a Storm 860 imager (Molecular Dynamics).

RNA Interference of MBD Protein

MBD1-specific siRNAs were designed and synthesized by Qiagen. Four different siRNA duplexes, recognizing four different sequences, were tested in HCT116 cells for their effectiveness to silence MBD1 expression. The most effective siRNA (Hs_MBD1_9: CGCGAAGTCTTTCGCAAGTCA) was selected for this study. A scramble siRNA (ATAGCGACTAAACACATCAA) was obtained from Dharmacon and used as control. Transfections were carried out using Lipofectamine (Invitrogen) according to the manufacturer's instructions and IFN-γ was added to the cell culture 48 h after transfection. The expression levels of MBD1 and IRF8 were analyzed by RT-PCR.

Disclosure of Potential Conflicts of Interest

No potential conflicts of interest were disclosed.

Acknowledgments

We thank Drs. V. Ganapathy and R. Markowitz for critical reading of the manuscript and Kimberly Smith for assistance in immunohistochemical staining of the human IRF8 protein in tumor tissues.

References

1. Contursi C, Wang IM, Gabriele L, et al. IFN consensus sequence binding protein potentiates STAT1-dependent activation of IFNγ-responsive promoters in macrophages. Proc Natl Acad Sci U S A 2000;97:91–6.

2. Holtschke T, Lohler J, Kanno Y, et al. Immunodeficiency and chronic myelogenous leukemia-like syndrome in mice with a targeted mutation of the ICSBP gene. Cell 1996;87:307–17.

3. Yang D, Thangaraju M, Greeneltch K, et al. Repression of IFN regulatory factor 8 by DNA methylation is a molecular determinant of apoptotic resistance and metastatic phenotype in metastatic tumor cells. Cancer Res 2007;67:3301–9.

4. Greeneltch KM, Schneider M, Steinberg SM, et al. Host immunosurveillance controls tumor growth via IFN regulatory factor-8 dependent mechanisms. Cancer Res 2007;67:10406–16.

5. Gabriele L, Phung J, Fukumoto J, et al. Regulation of apoptosis in myeloid cells by interferon consensus sequence-binding protein. J Exp Med 1999;190:411–21.

6. Middleton MK, Zukas AM, Rubinstein T, et al. Identification of 12/15-lipoxygenase as a suppressor of myeloproliferative disease. J Exp Med 2006;203:2529–40.

7. Schmidt M, Nagel S, Proba J, et al. Lack of interferon consensus sequence binding protein (ICSBP) transcripts in human myeloid leukemias. Blood 1998;91:22–9.

8. Liu K, Abrams SI. Coordinate regulation of IFN consensus sequence-binding protein and caspase-1 in the sensitization of human colon carcinoma cells to Fas-mediated apoptosis by IFN-γ. J Immunol 2003;170:6329–37.

9. Yang D, Thangaraju M, Browning DD, et al. IFN regulatory factor 8 mediates apoptosis in nonhemopoietic tumor cells via regulation of Fas expression. J Immunol 2007;179:4775–82.

10. Egwuagu CE, Li W, Yu CR, et al. Interferon-γ induces regression of epithelial cell carcinoma: critical roles of IRF-1 and ICSBP transcription factors. Oncogene 2006;25:3670–9.

11. Lee KY, Geng H, Ng KM, et al. Epigenetic disruption of interferon-γ response through silencing the tumor suppressor interferon regulatory factor 8 in nasopharyngeal, esophageal and multiple other carcinomas. Oncogene 2008;27:5267–76.

12. Kanno Y, Levi BZ, Tamura T, Ozato K. Immune cell-specific amplification of interferon signaling by the IRF-4/8-PU.1 complex. J Interferon Cytokine Res 2005;25:770–9.

13. Kanno Y, Kozak CA, Schindler C, et al. The genomic structure of the murine ICSBP gene reveals the presence of the γ interferon-responsive element, to which an ISGF3 α subunit (or similar) molecule binds. Mol Cell Biol 1993;13:3951–63.

14. Valente G, Ozmen L, Novelli F, et al. Distribution of interferon-γ receptor in human tissues. Eur J Immunol 1992;22:2403–12.

15. Darnell JE, Jr., Kerr IM, Stark GR. Jak-STAT pathways and transcriptional activation in response to IFNs and other extracellular signaling proteins. Science 1994;264:1415–21.

16. Ihle JN. STATs: signal transducers and activators of transcription. Cell 1996;84:331–4.

17. Bach EA, Aguet M, Schreiber RD. The IFN γ receptor: a paradigm for cytokine receptor signaling. Annu Rev Immunol 1997;15:563–91.

18. Decker T, Kovarik P, Meinke A. GAS elements: a few nucleotides with a major impact on cytokine-induced gene expression. J Interferon Cytokine Res 1997;17:121–34.

19. Rhee I, Bachman KE, Park BH, et al. DNMT1 and DNMT3b cooperate to silence genes in human cancer cells. Nature 2002;416:552–6.

20. Brattain MG, Fine WD, Khaled FM, Thompson J, Brattain DE. Heterogeneity of malignant cells from a human colonic carcinoma. Cancer Res 1981;41:1751–6.

21. Weisenberger DJ, Siegmund KD, Campan M, et al. CpG island methylator phenotype underlies sporadic microsatellite instability and is tightly associated with BRAF mutation in colorectal cancer. Nat Genet 2006;38:787–93.

22. Baylin SB, Ohm JE. Epigenetic gene silencing in cancer—a mechanism for early oncogenic pathway addiction? Nat Rev Cancer 2006;6:107–16.

23. Robertson KD. DNA methylation and human disease. Nat Rev Genet 2005;6:597–610.

24. Dawson DW, Hong JS, Shen RR, et al. Global DNA methylation profiling reveals silencing of a secreted form of Epha7 in mouse and human germinal center B-cell lymphomas. Oncogene 2007;26:4243–52.

25. Nelson WG, Yegnasubramanian S, Agoston AT, et al. Abnormal DNA methylation, epigenetics, and prostate cancer. Front Biosci 2007;12:4254–66.

26. Leu YW, Yan PS, Fan M, et al. Loss of estrogen receptor signaling triggers epigenetic silencing of downstream targets in breast cancer. Cancer Res 2004;64:8184–92.

27. Kerr KM, Galler JS, Hagen JA, Laird PW, Laird-Offringa IA. The role of

DNA methylation in the development and progression of lung adenocarcinoma. Dis Markers 2007;23:5–30.

28. Bird AP, Wolffe AP. Methylation-induced repression—belts, braces, and chromatin. Cell 1999;99:451–4.

29. Liu B, Liao J, Rao X, et al. Inhibition of Stat1-mediated gene activation by PIAS1. Proc Natl Acad Sci U S A 1998;95:10626–31.

30. Liu B, Mink S, Wong KA, et al. PIAS1 selectively inhibits interferon-inducible genes and is important in innate immunity. Nat Immunol 2004;5:891–8.

31. Rogers RS, Horvath CM, Matunis MJ. SUMO modification of STAT1 and its role in PIAS-mediated inhibition of gene activation. J Biol Chem 2003;278:30091–7.

32. Lyst MJ, Nan X, Stancheva I. Regulation of MBD1-mediated transcriptional repression by SUMO and PIAS proteins. EMBO J 2006;25:5317–28.

33. Laird PW. The power and the promise of DNA methylation markers. Nat Rev Cancer 2003;3:253–66.

34. Petak I, Danam RP, Tillman DM, et al. Hypermethylation of the gene promoter and enhancer region can regulate Fas expression and sensitivity in colon carcinoma. Cell Death Differ 2003;10:211–7.

35. Chen J, Rocken C, Lofton-Day C, et al. Molecular analysis of APC promoter methylation and protein expression in colorectal cancer metastasis. Carcinogenesis 2005;26:37–43.

36. Ebert MP, Model F, Mooney S, et al. Aristaless-like homeobox-4 gene methylation is a potential marker for colorectal adenocarcinomas. Gastroenterology 2006;131:1418–30.

37. Kim TY, Zhong S, Fields CR, Kim JH, Robertson KD. Epigenomic profiling reveals novel and frequent targets of aberrant DNA methylation-mediated silencing in malignant glioma. Cancer Res 2006;66:7490–501.

38. Chan MW, Wei SH, Wen P, et al. Hypermethylation of 18S and 28S ribosomal DNAs predicts progression-free survival in patients with ovarian cancer. Clin Cancer Res 2005;11:7376–83.

39. Goll MG, Bestor TH. Eukaryotic cytosine methyltransferases. Annu Rev Biochem 2005;74:481–514.

40. Liu K, McDuffie E, Abrams SI. Exposure of human primary colon carcinoma cells to anti-Fas interactions influences the emergence of pre-existing Fas-resistant metastatic subpopulations. J Immunol 2003;171:4164–74.

41. Flatmark K, Maelandsmo GM, Martinsen M, Rasmussen H, Fodstad O. Twelve colorectal cancer cell lines exhibit highly variable growth and metastatic capacities in an orthotopic model in nude mice. Eur J Cancer 2004;40:1593–8.

42. Cespedes MV, Espina C, Garcia-Cabezas MA, et al. Orthotopic microinjection of human colon cancer cells in nude mice induces tumor foci in all clinically relevant metastatic sites. Am J Pathol 2007;170:1077–85.

43. Boyd D, Florent G, Kim P, Brattain M. Determination of the levels of urokinase and its receptor in human colon carcinoma cell lines. Cancer Res 1988;48:3112–6.

44. Tate PH, Bird AP. Effects of DNA methylation on DNA-binding proteins and gene expression. Curr Opin Genet Dev 1993;3:226–31.

45. Boyes J, Bird A. DNA methylation inhibits transcription indirectly via a methyl-CpG binding protein. Cell 1991;64:1123–34.

46. Murray EJ, Grosveld F. Site specific demethylation in the promoter of human γ-globin gene does not alleviate methylation mediated suppression. EMBO J 1987;6:2329–35.

47. Fatemi M, Wade PA. MBD family proteins: reading the epigenetic code. J Cell Sci 2006;119:3033–7.

48. Yang D, Stewart TJ, Smith KK, Georgi D, Abrams SI, Liu K. Down-regulation of IFN-γR in association with loss of Fas function is linked to tumor progression. Int J Cancer 2008;122:350–62.

49. Yang D, Ud Din N, Browning DD, Abrams SI, Liu K. Targeting lymphotoxin β receptor with tumor-specific T lymphocytes for tumor regression. Clin Cancer Res 2007;13:5202–10.

50. Liu K, Catalfamo M, Li Y, Henkart PA, Weng NP. IL-15 mimics T cell receptor crosslinking in the induction of cellular proliferation, gene expression, and cytotoxicity in $CD8^+$ memory T cells. Proc Natl Acad Sci U S A 2002;99:6192–7.

51. Andrews NC, Faller DV. A rapid micropreparation technique for extraction of DNA-binding proteins from limiting numbers of mammalian cells. Nucleic Acids Res 1991;19:2499.

Molecular Cancer Research

DNA Methylation Represses IFN-γ–Induced and Signal Transducer and Activator of Transcription 1–Mediated IFN Regulatory Factor 8 Activation in Colon Carcinoma Cells

Jon M. McGough, Dafeng Yang, Shuang Huang, et al.

Mol Cancer Res 2008;6:1841-1851.